Int J Adv Manuf Technol (2009) 42:813–821
DOI 10.1007/s00170-008-1643-x

ORIGINAL ARTICLE

Functional simulator of 3-axis parallel kinematic milling machine

Milos Glavonjic · Dragan Milutinovic · Sasa Zivanovic

Received: 12 July 2007 / Accepted: 27 June 2008 / Published online: 24 July 2008

Abstract Parallel kinematic machines (PKM) are research-and-development topic in many laboratories although many of them, unfortunately, have no PKM at all. Therefore, the use of low cost but functional simulator of a 3-Axis parallel kinematic milling machine is suggested as a help to acquire the basic experiences in the PKM field. The idea is based on the possibility that the simulator could be driven and controlled by a conventional 3-Axis Computer Numerical Control machine tool (CNC). The paper describes the development procedure of a simulator including the selection of a corresponding parallel mechanism, kinematic modelling, and the programming algorithm. The functional simulator idea has been verified by successful making of some standardized test pieces of soft material, under full operational conditions.

Keywords Parallel kinematic machines · Functional simulator · Modelling and testing

1 Introduction

The strategic importance of education and training, especially in technology and scientific subjects, is growing throughout the world. This also applies to the parallel kinematic machines (PKMs) which are today research-and-development (R&D) and educational worldwide topic. Basic knowledge about diverse aspects of PKM has been published [1]. Many different topologies of parallel mechanisms with 3 to 6 *dof*, including a 3-*dof* translational orthogonal parallel mechanism, have been used [1–5]. Today, unfortunately, the great majority of research institutes, university laboratories, and companies have no PKM. The reason, obviously, is the high cost of education and training for a new technology, such as PKM.

In order to contribute towards the acquisition of practical experiences in modelling, design, control, programming, and the use of PKM, a low cost but functional simulator of 3-Axis parallel kinematic milling machine is proposed [2]. The idea is based on the possibility that the simulator could be driven and controlled by a conventional 3-Axis CNC machine tool.

As the axes of the conventional 3-Axis CNC machine are mutually orthogonal, different 3-*dof* spatial parallel mechanisms with orthogonal translatory joints may be used to build the simulator [2, 7].

The paper describes the procedure for simulator development including the selection of a corresponding parallel mechanism, kinematic modelling, and the programming algorithm. The idea about the functional simulator was verified by successful making of some standardized test pieces out of soft materials, made under full operational conditions.

2 Simulator's concept

It would be possible, thanks to the previous knowledge about serial kinematic machines and available resources for their programming, to make the simulator as a hybrid structure consisting of driving conventional 3-Axis CNC milling machine and driven 3-*dof* spatial parallel mechanism. One of the possible concepts of a functional simulator

M. Glavonjic (✉) · D. Milutinovic · S. Zivanovic
Mechanical Engineering Faculty, University of Belgrade,
Kraljice Marije 16,
11120 Belgrade, Serbia
e-mail: mglavonjic@mas.bg.ac.yu

for 3D milling of softer materials, shown in Fig. 1, consists of:

- Fully parallel 3-*dof* mechanism with constant strut lengths and linear joints actuated and controlled by the conventional 3-Axis CNC machine. The mechanism is based on linear DELTA mechanism [6] but with orthogonal linear actuated joints to facilitate its connection with X_M, Y_M, and Z_M axes of horizontal or vertical serial kinematic machines. The universal platform, which always remains parallel with the base, enables the placement of the spindle in three different orthogonal X_P, Y_P, $-Z_P$ directions as shown in Fig. 1. Out of several possible configurations of the mechanism, the one with the platform inside the trihedron (X_B, Y_B, $-Z_B$) has been selected since it enables easy mounting of the parallel mechanism on the serial machine X_M axis guideways.
- Serial 2-*dof* passive mechanism for decoupling serial machine's Y_M and Z_M axes.

In addition to the selection and adjustment of the simulator's mechanism with the chosen serial machine, the following procedures, models, algorithms, and software have to be defined and developed:

– kinematic modelling of parallel mechanism, i.e., inverse and direct kinematics, Jacobian matrices, and singularity analysis,
– workspace analysis and selection of simulator proper design parameters,
– simulator design and manufacturing,

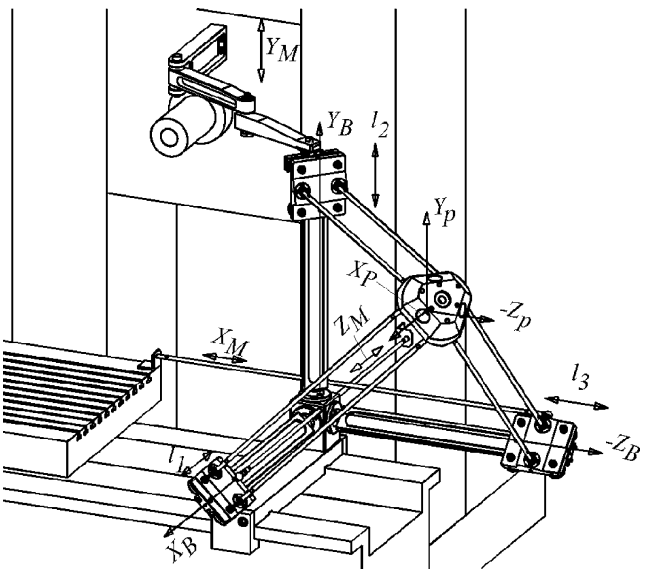

Fig. 1 Functional simulator concept

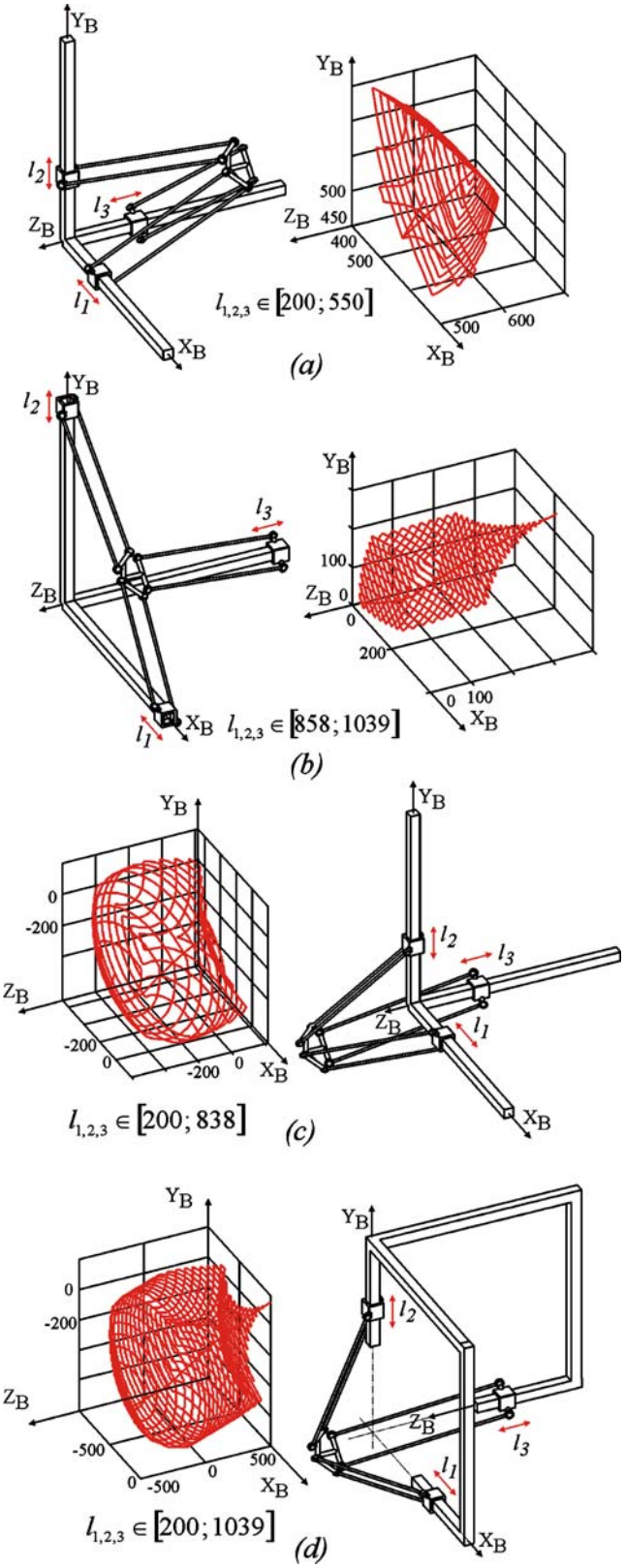

Fig. 2 The basic concepts of simulator's parallel mechanism

– the procedure and accessories for adjustment of parallel mechanism's referent points to simplify the programming,
– algorithms and software for simulator programming,
– the procedure for testing of simulator under working conditions by machining of various test pieces from softer materials.

3 On simulator mechanisms

As the axes of the vertical and horizontal 3-Axis CNC serial machines are orthogonal and actuating simulator's axes at the same time, it would be the best if 3-*dof* spatial parallel simulator's mechanism has orthogonal translatory joints as well. As in serial CNC machines the axes are coupled, it would be essential, in a general case, to have at least one 2-*dof* passive serial mechanism for their decoupling. The most convenient CNC machine tools for the simulator are those with movable tool holder and working table. In such concepts two out of three axes are coupled so that one 2-*dof* serial passive mechanism suffices for their decoupling and the actuation of the simulator.

Without classification of kinematic structures of horizontal and vertical 3-Axis CNC machines, some examples of 3-*dof* spatial parallel mechanisms with orthogonal translatory joints, which have been considered and used for the simulator, are presented in Fig. 2. The shapes of their workspaces are shown as well in the figure.

The above and similar examples of the mechanism are the result of the solution variances of the inverse and direct kinematic problem of the basic concept illustrated in Fig. 1.

The examples of 2-*dof* passive serial mechanisms used to decouple the motion of the axes of driving serial CNC machine are shown in Fig. 3.

In some serial CNC machine concepts, their axes may be directly used as simulator's parallel mechanism translatory joints. In such cases, the general concept of the simulator based on mechanisms shown in Fig. 2 may be simplified.

Figure 4 shows an example of the simplified simulator with parallel mechanism without its own joints. The driving serial CNC machine is a horizontal machining center. The

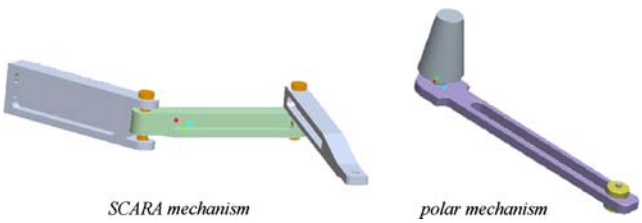

Fig. 3 The examples of serial mechanisms for decoupling of driving machine's axes

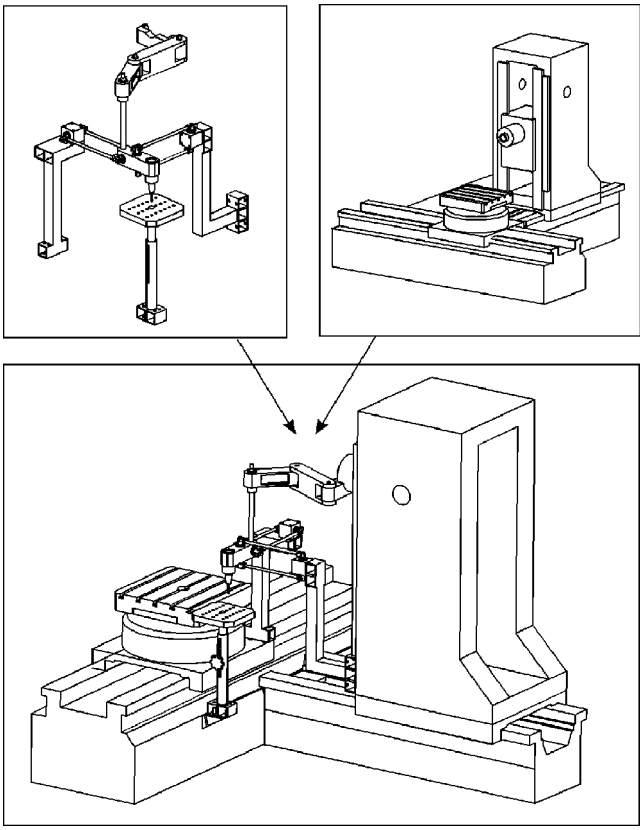

Fig. 4 The example of the simulator without own translatory joints

corresponding mechanical interfaces connect joint parallelograms with decoupled axes of the machining centre. 2-*dof* serial mechanism decouples machining center's *Y* and *Z* axes.

Figure 5 shows the design of a simplified simulator for a vertical CNC milling machine with two coupled axes. Simulator's mechanism has one own translatory joint while 2-*dof* serial mechanism is also used for decoupling of the vertical CNC milling machine axes.

4 Simulator modelling example

Detailed kinematic analysis of the simulator from Fig. 1, is based on its geometric model, Fig. 6. As the platform, by mechanism's nature, remains parallel with the base, each spatial parallelogram, Fig. 1, is represented by one strut.

The fact that the coordinate frames, $\{B\}$ and $\{P\}$, connected to the base and the platform are parallel and that they are, at the same time, parallel with the referent serial machine coordinate frame $\{M\}$ enables generalization of the modelling of the entire simulator. This means that it is feasible to separate the modelling of the parallel mechanism itself, regardless of its mounting on the horizontal or vertical serial machine and the position of the spindle on

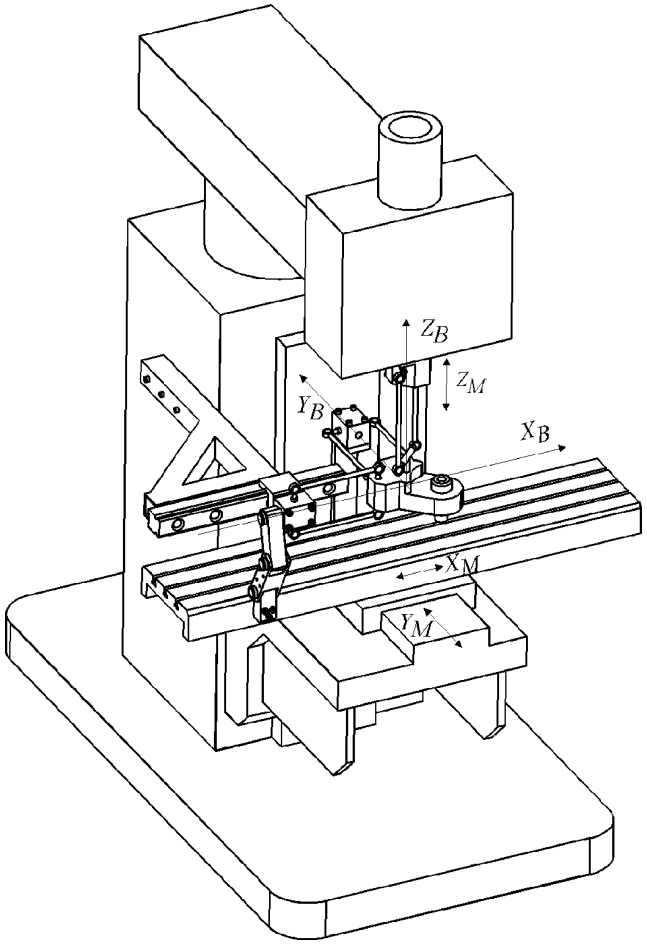

Fig. 5 Example of a simulator on the vertical CNC milling machine

its platform. Vectors **v** referenced in frames $\{B\}$ and $\{P\}$ are denoted by ${}^{B}\mathbf{v}$ and ${}^{P}\mathbf{v}$.

Vectors defined by simulator parameters:

- The position vectors of the midpoints C_i between joint centers at mobile platform are defined in the frame $\{P\}$ as, ${}^{P}\mathbf{P}_{Ci}, (i = 1, 2, 3)$.
- The position vector of the tool tip is defined in the frame $\{P\}$ as ${}^{P}\mathbf{P}_{T}, [x_{TP}\, y_{TP}\, z_{TP}]^T$, where $z_{TP} = -h$.
- The position vectors of simulator's driving axes reference points R_i are defined as, ${}^{B}\mathbf{P}_{Ri}, (i = 1, 2, 3)$.

Joint coordinates vector:

- $\boldsymbol{l} = [l_1\, l_2\, l_3]^T$, l_1,l_2, and l_3 are scalar variables powered and controlled by serial CNC machine within the range of $l_{\min} \le l_i \le l_{\max}$, while ${}^{B}\mathbf{a}_i$ are unit vectors, ${}^{B}\mathbf{a}_1 = [1\ 0\ 0]^T$, ${}^{B}\mathbf{a}_2 = [0\ 1\ 0]^T$ and ${}^{B}\mathbf{a}_3 = [0\ 0\ -1]^T$.

World coordinates vector:

${}^{B}\mathbf{P}_T = [x_T\, y_T\, z_T]^T$ represents the programmed position vector of the tool tip, while $\boldsymbol{x} = {}^{B}\mathbf{P}_{OP} = [x_p\, y_p\, z_p]^T$ represents the location of the platform, i.e., the origin O_p of the coordinate frame $\{P\}$ attached to it. The relationship between these two vectors is obvious since coordinate frames $\{B\}$ and $\{P\}$ are always parallel, i.e.,

$$ {}^{B}\mathbf{P}_T = {}^{B}\mathbf{P}_{OP} + {}^{P}\mathbf{P}_T \tag{1} $$

Other vectors and parameters are defined as shown in Fig. 6, where ${}^{B}\mathbf{w}_i$ and ${}^{B}\mathbf{q}_i$ are unit vectors while c is fixed length of joint parallelograms.

The relationships between the simulator's joint coordinates vector $\boldsymbol{l} = [l_1\ l_2\ l_3]^T$ and the serial machine joint coordinates $\mathbf{m} = [x'_M y_M z_M]^T$, as shown in Fig. 6, are:

$$ x'_M = l_3, \quad y_M = l_2, \quad z_M = -1_1 \tag{2} $$

On the basis of geometric relations shown in the Fig. 6, the following equations are derived:

$$ k_i^B \mathbf{w}_i = {}^{B}\mathbf{P}_{OP} + {}^{P=B}\mathbf{P}_{Ci} - {}^{B}\mathbf{P}_{Ri} \tag{3} $$

$$ k_i^B \mathbf{w}_i = l_i^B \mathbf{a}_i + c^B \mathbf{q}_i \tag{4} $$

By taking the square of both sides in Eq. 4 the following relation is derived:

$$ c^2 = k_i^2 + l_i^2 - 2l_i\left({}^{B}\mathbf{a}_i k_i^B \mathbf{w}_i\right) \tag{5} $$

By adopting

$$ {}^{P=B}\mathbf{P}_{Ci} - {}^{B}\mathbf{P}_{Ri} = 0 \tag{6} $$

in Eq. 3, kinematic modelling is very simplified. In order to fulfill this requirement, specific calibration method, i. e., setting of reference points R_i has been developed. By

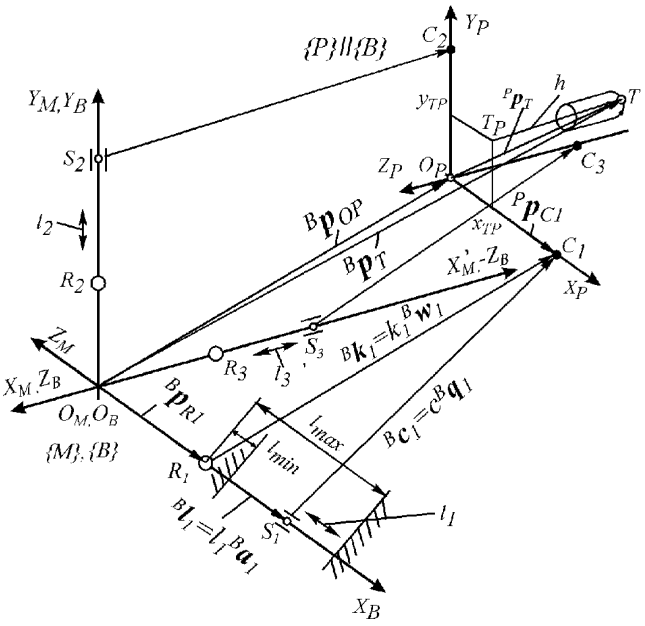

Fig. 6 Geometric model of the simulator

substituting other mechanism's parameters in Eq. 5, the system of the following three equations is obtained

$$\begin{cases} x_p^2 + y_p^2 + z_p^2 + l_1^2 - 2l_1x_p - c^2 = 0 \\ x_p^2 + y_p^2 + z_p^2 + l_2^2 - 2l_2y_p - c^2 = 0 \\ x_p^2 + y_p^2 + z_p^2 + l_3^2 + 2l_3z_p - c^2 = 0 \end{cases} \quad (7)$$

from which are derived:

– inverse kinematic equations as

$$\begin{cases} l_1 = x_p \pm \sqrt{c^2 - y_p^2 - z_p^2} \\ l_2 = y_p \pm \sqrt{c^2 - x_p^2 - z_p^2} \\ l_3 = -z_p \pm \sqrt{c^2 - x_p^2 - y_p^2} \end{cases} \quad (8)$$

as well as

– direct kinematic equations as

$$\begin{cases} y_p = \frac{-s_6 \pm \sqrt{s_6^2 - 4s_5s_7}}{2s_5} \\ x_p = s_1 + s_2y_p \\ z_p = s_3 + s_4y_p \end{cases} \quad (9)$$

where are

$$s_1 = \frac{l_1^2 - l_2^2}{2l_1}, s_2 = \frac{l_2}{l_1}, s_3 \frac{l_2^2 - l_3^2}{2l_3}, s_4 = -\frac{l_2}{l_3},$$
$$s_5 = 1 + s_2^2 + s_4^2,\ s_6 = 2(s_1s_2 + s_3s_4 - l_1s_2),$$
$$s_7 = s_1^2 + s_3^2 - 2l_1s_1 - c^2 + l_1^2,\ l_{\min} \le l_i \le l_{\max}, i = 1, 2, 3$$

As it was mentioned, by adjustment of simulator's mechanism parameters, Eq. 6, the solution of inverse and direct kinematics is greatly simplified. To satisfy the conditions from Eq. 6 six calibration struts of selected referent length were used, Fig. 7. With the use of inverse and direct kinematics solutions with the calibrated strut lengths, the positions of reference points R_i of sliders S_i, (i= 1, 2, 3) are defined and fixed by calibration plain rings, Fig. 7.

4.1 The analysis of inverse and direct kinematics solutions

With the analysis of inverse kinematics variance solutions, Eq. 8, different configurations of parallel mechanism for a given platform position may be noted:

– the basic configuration, Fig. 2a, when in the Eq. 8, all signs before the square root are negative,
– one of alternative configurations, Fig. 2b, when in Eq. 8, all signs before square root are positive,
– other possible mechanism configurations, when in the Eq. 8, signs before the square root are combined.

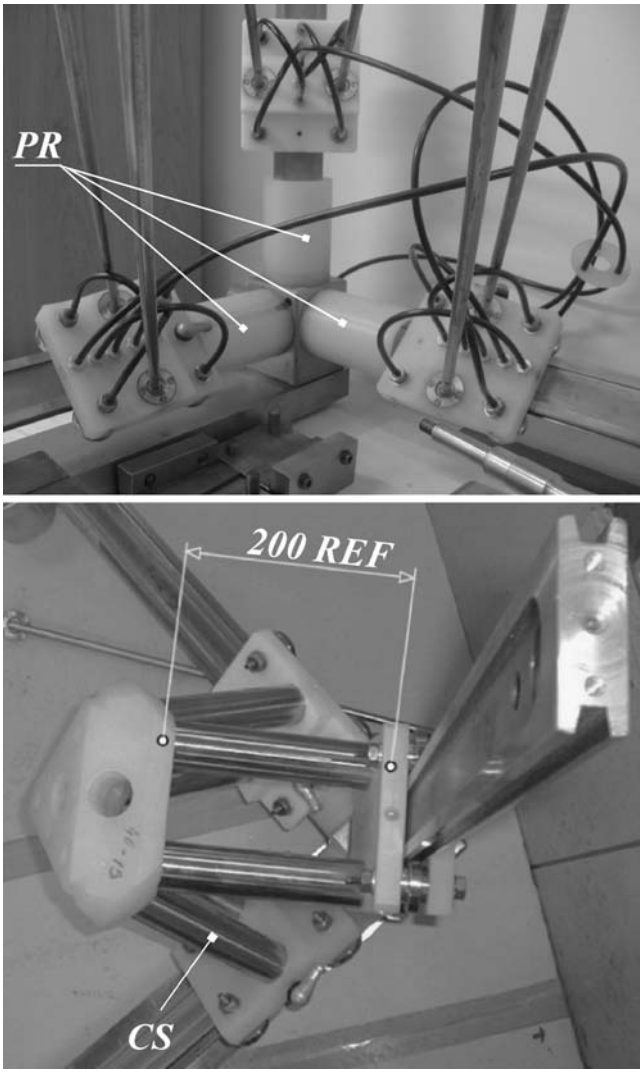

Fig. 7 Setting of simulator's reference points

In a similar way, through the analysis of direct kinematic solution, Eq. 9, different configurations of parallel mechanism for given positions of driving axes may be established:

– the basic configuration, Fig. 2a, corresponding to the case, when in Eq. 9, there is a positive sign before square root,
– alternative configurations, Figs. 2c and d, when in Eq. 9, there is a negative sign before square root.

The basic and alternative configurations shown in Fig. 2 may be realized in different ways subject to the structure of the driving serial machine.

4.2 Jacobian matrices and singularity analysis

In view of the significance of PKM singularity, this problem has been analyzed in detail for the mechanism variant shown in Fig. 2a, used for the development of the

simulator on horizontal machining center, Fig. 1. Differentiating Eq. 8 with respect to the time, Jacobian matrix is obtained as

$$\mathbf{J} = \begin{bmatrix} 1 & \frac{y_p}{x_p - l_1} & \frac{z_p}{x_p - l_1} \\ \frac{x_p}{y_p - l_2} & 1 & \frac{z_p}{y_p - l_2} \\ -\frac{x_p}{z_p + l_3} & -\frac{y_p}{z_p + l_3} & -1 \end{bmatrix} \tag{10}$$

As the equations in Eq. 7 are implicit functions of joint and world coordinates, Jacobian matrix may be also obtained by their differentiation as

$$\mathbf{J} = \mathbf{J}_l^{-1} \cdot \mathbf{J}_x \tag{11}$$

where

$$\mathbf{J}_l^{-1} = \frac{1}{2} \begin{bmatrix} \frac{1}{x_p - l_1} & 0 & 0 \\ 0 & \frac{1}{y_p - l_2} & 0 \\ 0 & 0 & -\frac{1}{z_p + l_3} \end{bmatrix} \tag{12}$$

$$\mathbf{J}_x = 2 \begin{bmatrix} x_p - l_1 & y_p & z_p \\ x_p & y_p - l_2 & z_p \\ x_p & y_p & z_p + l_3 \end{bmatrix} \tag{13}$$

are Jacobian matrices of inverse and direct kinematics.

In this way, three different types of singularities can be identified, e.g., singularities of inverse and direct kinematics as well as combined singularities.

With careful analysis of Jacobian matrices determinants

$$\det(\mathbf{J}) = \frac{x_p l_2 l_3 + y_p l_1 l_3 - z_p l_1 l_2 - l_1 l_2 l_3}{(x_p - l_1)(y_p - l_2)(z_p + l_3)} \tag{14}$$

$$\det(\mathbf{J}_x) = -8\left(x_p l_2 l_3 + y_p l_1 l_3 - z_p l_1 l_2 - l_1 l_2 l_3\right) \tag{15}$$

$$\det(\mathbf{J}_l) = -8(x_p - l_1)(y_p - l_2)(z_p + l_3) \tag{16}$$

the singularities of inverse and direct kinematics as well as combined singularity may be noticed.

Figure 8 shows these possible simulator's singularity configurations with corresponding descriptions and equations. As it can be seen from Fig. 8, all singularities are on the borders of theoretically achievable workspace so that it would be possible to avoid them easily with adequate design solutions and/or mechanical constrains. This means that the achievable simulator's workspace is smaller than theoretical workspace. The boundaries of theoretical workspace are on cylinders of radius c whose axes are X_B, Y_B, $-Z_B$ derived from inverse kinematic Eq. 8 and sphere of radius c centered in O_B, Fig. 8.

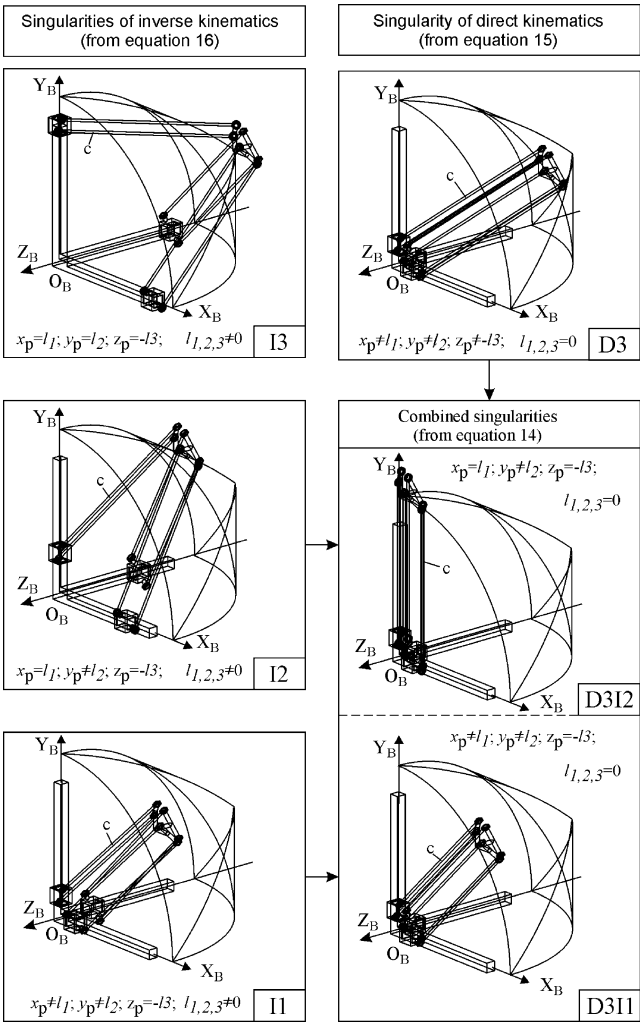

Fig. 8 Singularity types

5 The examples of simulators

As it is known in addition to selecting appropriate kinematic topology, the selection of the right geometric dimensions is very important since the performance is highly influenced by PKM geometric dimensions [1, 8].

To select the right dimensions with respect to a given application is a difficult task, and the development of design tools for PKM is still open research [1].

The design parameters of simulators shown in Figs. 1, 4, and 5 were adjusted in order to get more adequate shapes and workspace dimensions on the basis of performances of available CNC machines for which simulators were planned. The procedure is essentially iterative because in determination of the basic design parameters the attention is paid to the possible interferences of structural elements and the values of $\det(\mathbf{J})$ and $\det(\mathbf{J}^{-1})$ determinants, Eqs. 14, 15, and 16.

In the geometric model of simulator variant from Fig. 6, it can be seen that workspace dimensions are primarily affected by parallelograms length c, as well as to the adequacy of the distance of the mechanism from D3, D3I2, and D3I1 singularities shown in Fig. 8.

For available CNC machine for which the simulator was planned, parallelograms length c and values joint of coordinates $l_{1,2,3\min}$ and $l_{1,2,3\max}$ were analyzed in iterative procedure. In each iteration, attention was paid to the potential design limitations, interferences, as well as to the values of det($\mathbf{J}$) and det($\mathbf{J}^{-1}$), i.e., to the distances from singularities.

The parameters determined in this way have been slightly corrected in detailed design of the simulator prototype shown in Fig. 9. Shape, volume, and position of achievable workspace for parallelograms length c=850 mm and $l_{1,2,3\min}$=200 mm and $l_{1,2,3\max}$=550 mm are shown in Fig. 2a.

On the basis of the adopted concepts and design parameters, the first two simulators have been built (Figs. 9 and 10).

6 Simulator programming and testing

The simulator programming system has been developed in a standard CAD–CAM environment on PC platform (Fig. 11). It is possible to exchange geometric workpiece models with other systems and simulate the tool path. Linear interpolated tool path is taken from the standard CL file. The tool path may also be generated in some other way selected by the simulator user. The basic part of the system consists of developed and implemented postprocessor, without the use of postprocessor generator. The postprocessor contains inverse and direct kinematics, simulator

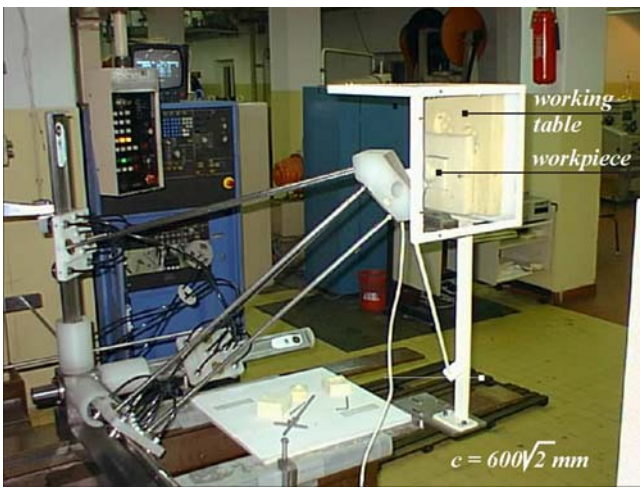

Fig. 9 Completed simulator from Fig. 1

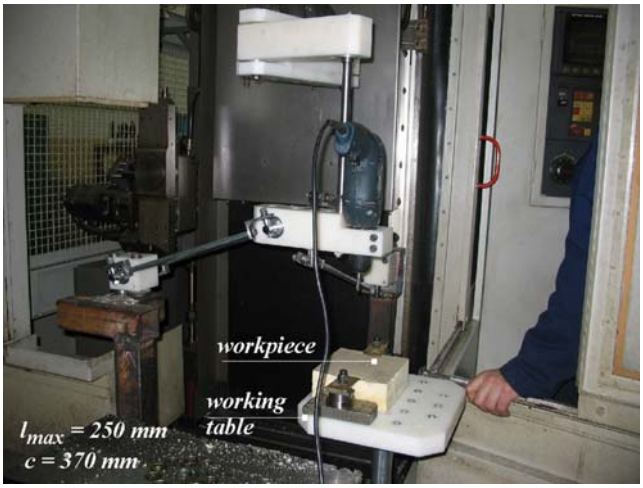

Fig. 10 Completed simulator from Fig. 4

design parameters, and algorithm for simulator's tool path linearization (Fig. 12). Simulator's tool path linearization is essential because CNC machine's linear interpolation is used as simulator's joint coordinates interpolation. In this way, simulator's tool path remains within the tolerance tube of predefined radius between points T_{j-1} and T_j taken from CL file. The long program for CNC machine obtained in

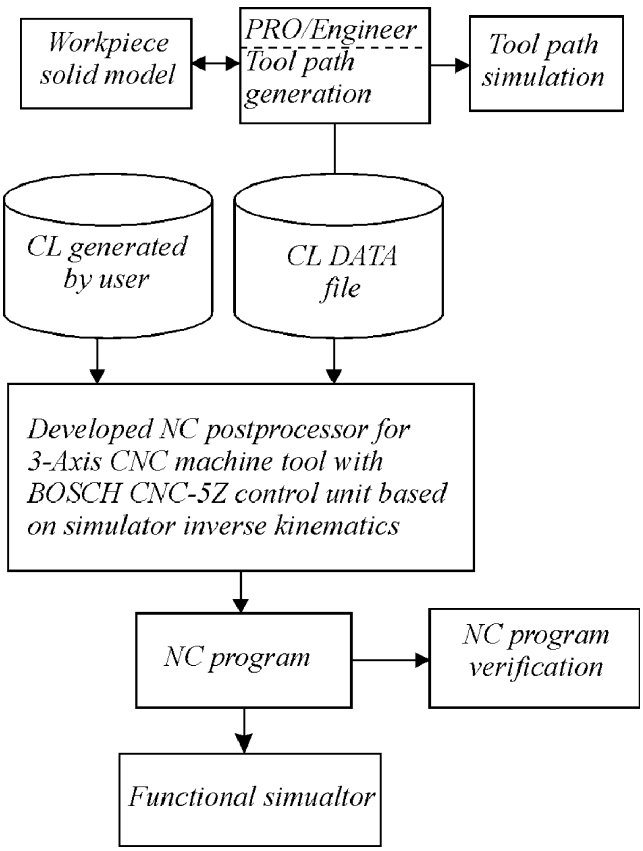

Fig. 11 Simulator programming system

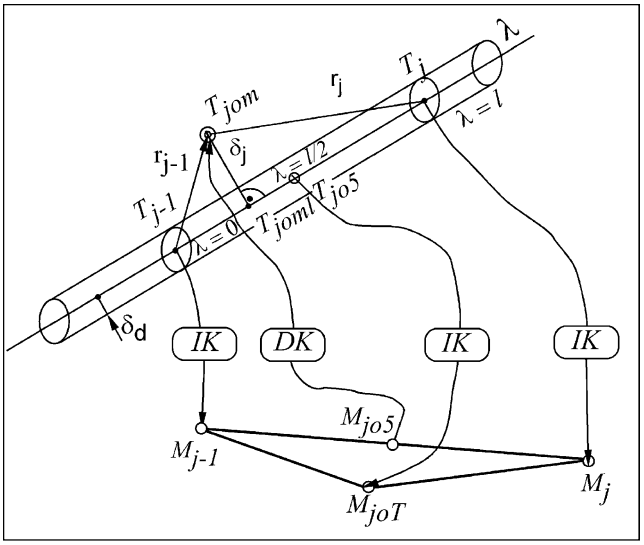

IK: inverse kinematic DK: direct kinematic

$\overline{T_{j-1}T_j}$: *chord from CL file*

$\overline{M_{j-1}M_j}$: *driving machine's path segment*

Linearization Algorithm:

K1: *Set* T_{j-1} *and* T_j *from CL file, or from current iteration step.*

K2: $IK(T_{j-1}) \longrightarrow M_{j-1}$, $IK(T_j) \longrightarrow M_j$.

K3: M_{jo5} *: middle point of* $\overline{M_{j-1}M_j}$,

$DK(M_{jo5}) \longrightarrow T_{jom}$.

K4: T_{joml} *: Projection of* T_{jom} *onto* $\overline{T_{j-1}T_j}$.

If $\lambda < 0$, *then* $\delta = \max(r_{j-1}, \delta_j)$

else $0 \le \lambda \le l$, *then* $\delta = \delta_j$

else $\lambda > l$ *then* $\delta = \max(r_j, \delta_j)$.

K6: *If* $\delta \le \delta_d$ *then chord* $\overline{T_{j-1}T_j}$ *satisfies linearization.*

If $\delta > \delta_d$, *then insert new point* T_{jo5} *in the middle of* $\overline{T_{j-1}T_j}$, *calculate* $M_{joT} = IK(T_{jo5})$ *and create new chords* $\overline{M_{j-1}M_{joT}}$ *and* $\overline{M_{joT}M_j}$.

Go to ***K1***.

Fig. 12 Uniform linearization of simulator's tool path

this way is transferred to CNC machine and can be verified during idle running of the simulator. The motion range of driving axes has been already checked in the postprocessor.

The testing of the simulator in this phase included:

- verification of the system for programming and communication, and
- cutting tests by machining various test pieces (Fig. 13).

7 Conclusion

In order to contribute towards the acquisition of practical experiences in modelling, design, control, programming, and the use of PKM, a low cost but functional simulator of 3-Axis parallel kinematic milling machine is proposed. The developed functional simulator of the 3D parallel kinematic milling machine integrates, as a hybrid system, the existing technological equipment (CNC machine tools, CAD–CAM hardware and software) and parallel kinematic mechanism into a comprehensive and sophisticated didactic facility. The idea about the functional simulator was verified by successful making of some standardized test pieces out of soft materials, made under full operational conditions. Its capabilities and characteristics have shown that the simulator itself was an interesting and valuable R&D topic. This idea may be further used for making of one's own simulators.

Fig. 13 Test pieces made of foam

Acknowledgements The presented work was part of Eureka project E!3239 supported by the Ministry of Science of Serbia.

References

1. Weck M, Staimer D (2002) Parallel kinematic machine tools—current state and future potentials. CIRP Annals—Manufacturing Technology 51(2):671–683 doi:10.1016/S0007-8506(07)61706-5
2. Covic N (2000) The development of the conceptual design of class of flexible manufacturing systems. University of Belgrade, Belgrade Faculty of Mechanical Engineering, Dissertation, in Serbian
3. Chablat D, Wenger P (2003) Architecture optimization of a 3-*dof* translational parallel mechanism for machining applications, the Orthoglide. IEEE Trans Robot Autom 19:403–410 doi:10.1109/TRA.2003.810242
4. Pashkevich A, Chablat D, Wenger P (2006) Kinematics and workspace analysis of a three-axis parallel manipulator: the Orthoglide. Robotica 24:39–49 doi:10.1017/S0263574704000347
5. Kim HS, Tsai LW (2003) Design optimization of a cartesian parallel manipulator. J Mech Des 125:43–51 doi:10.1115/1.1543977
6. Demaurex MO (1999) The Delta Robot Within Industry. In: Boer CR et al (ed) Parallel kinematic machines, theoretical aspects and industrial requirements. Springer, London, pp 395–399 ISBN 1852336137
7. Glavonjic M, Milutinovic D, Zivanovic S, Bouzakis K, Mitsi S, Misopolinos L (2005) Development of a Parallel Kinematic Device Integrated into a 3-axis Milling Centre. Proc 2nd International Conference on Manufacturing Engineering ICMEN and EUREKA Brokerage Event, Kassandra-Chalkidiki, Greece, pp 351–361
8. Milutinovic D, Glavonjic M, Kvrgic V, Zivanovic S (2005) A new 3-*dof* spatial parallel mechanism for milling machines with long X travel. CIRP Annals—Manufacturing Technology 54(1):345–348 doi:10.1016/S0007-8506(07)60119-X